

# Late autumn aerosol trace element composition and source tracking over the southern Mozambique Channel

Morgane M.G. Perron<sup>1</sup>, Eva Bucciarelli<sup>1</sup>, H el ene Planquette<sup>1</sup>, Thomas Holmes<sup>2</sup>, Saumik Samanta<sup>3,4</sup>, Yoan Germain<sup>5</sup>, Alakendra Roychoudhury<sup>4</sup>, G eraldine Sarthou<sup>1</sup>.

5 <sup>1</sup> Univ Brest, CNRS, IFREMER, IRD, LEMAR, IUEM, F-29280 Plouzan e, France

<sup>2</sup> Australian Antarctic Program Partnership (AAPP), University of Tasmania, Battery Point, Tasmania, Australia

<sup>3</sup> School of Geosciences, University of the Witwatersrand, Johannesburg, South Africa

<sup>4</sup> Department of Earth Sciences, Stellenbosch University, Stellenbosch, South Africa

<sup>5</sup> IFREMER, CNRS, Univ Brest, UBS, UMR6538, Laboratoire Geo-Ocean, F-29280 Plouzan e, France

10 Correspondence to: Morgane M. G. Perron (morgane.perron@univ-brest.fr)

## Abstract.

The southern Mozambique Channel (20-30  S) receives a range of atmospheric influences, from desert dust and fire emissions through to industrial, mining and agricultural emissions, emitted from both Madagascar and southeastern Africa. Our study characterises the trace element composition of aerosols collected between the south of Madagascar and Durban, South Africa during the low dust season. Dust deposition fluxes (40-263 mg m<sup>-2</sup> yr<sup>-1</sup>), calculated based on Al measurement in aerosols, fell within the lower range of modelled fluxes estimates, confirming the absence of major dust or fire events during the study. While prevailing air-masses affecting our samples were modelled to originate from long-range particulate transport over the Southern Ocean, a holistic understanding of our sample composition could only be obtained when accounting for sporadic aeolian inputs from the two local landmasses. Notably, we found surprising high levels of Cr (4±2 ng m<sup>-3</sup>) and Cd (0.02±0.01 ng m<sup>-3</sup>) in the atmosphere over the southern Channel which could be, at least in part, attributed to emissions from mining (chromite and gold, respectively) and smelting activities (Cu, Zn and Cd co-emission) on both neighbouring landmasses. Our results emphasise the difficulty to track such specific and overlooked atmospheric sources in the absence of known atmospheric tracers. We also stress the need for multi-elemental studies and encourage the use of detailed (cluster) air-mass transport model analysis in regions dominated by the long-range atmospheric transport as complex atmospheric circulation and minor (sporadic) inputs from terrestrial air-masses may have disproportionate impact on the atmospheric composition.

15  
20  
25

## 30 1 Introduction

Atmospheric transport and deposition of trace elements play a key role in shaping marine biogeochemical cycles. In particular, iron (Fe) delivered via dust inputs can stimulate primary productivity in nutrient-limited oceanic regions, thereby modulating the marine carbon cycle (Mendez et al., 2010). Conversely, aeolian deposition can also introduce potentially toxic elements such as

35 cadmium (Cd), copper (Cu), lead (Pb) and zinc (Zn), emitted from urban and industrial areas, which can  
be deleterious for coastal marine ecosystems (Paytan et al., 2009; Thiagarajan et al., 2024; Zhou et al.,  
2021). Determining the relative contribution of these various sources, as well as their chemical  
composition is thus essential to assess their ecological impact.

The southern Mozambique Channel (defined between 20° S-30° S in this study) lies between two  
40 landmasses, namely the island of Madagascar to the east and the southeastern coast of Africa (including,  
South Africa and Mozambique) to the west. Both landmasses are characterised by arid to semi-arid  
landscapes which are increasingly prone to droughts (Barimalala et al., 2024; Mahlalela et al., 2020;  
Rigden et al., 2024) and wildfires (Frappier-Brinton and Lehman, 2022; Richardson et al., 2022; Swap  
et al., 2002, 2003). The dry season runs from May to October and corresponds to the most favourable  
45 period for dust entrainment into the atmosphere and long-range transport towards open ocean areas  
(Bhattachan et al., 2012; Ginoux et al., 2012).

Earth system models and satellite observations consistently identify the Namib Desert, the Etosha basin  
in Namibia, the Kalahari Desert in Botswana as well as local ephemeral rivers (Bhattachan et al., 2015)  
as major dust sources in Southern Africa. Seasonally, these sources contribute significantly to dust  
50 deposition across sub-tropical (25° S-40° S) latitudes of the southwest Indian Ocean (Gili et al., 2022;  
Jickells et al., 2005; Li et al., 2008a). In addition, during the dry season, savannah fires in southern  
Africa emit large plumes of nutrient-rich smoke, forming a “river of smoke” that can extend eastwards  
across the Mozambique Channel and even reach western Australia (Ranaivombola et al., 2025; Swap  
et al., 2002, 2003). Recently, southern Africa iron-rich dust has been linked to the formation of unusually  
55 large phytoplankton blooms in the southern Mozambique Channel south of Madagascar (Gittings et al.  
2024). More locally, atmospheric transport from Madagascar has also been demonstrated across the  
Mozambique Channel during the dry season (Kumar et al., 2014).

From the 21<sup>st</sup> century on, intensification of land use, including agriculture, mining, transport and  
urbanization, has resulted in the doubling of dust emissions from southern Africa and Madagascar  
60 Island (Hooper and Marx, 2018). In addition, South Africa is the 7<sup>th</sup> largest coal-producing and coal-  
consuming country in the world. The production (mining) and use of coal, be it for industries, energy  
production or for domestic burning, results in emissions of airborne hazardous volatile particles (such as  
lead, Pb, cadmium, Cd, or mercury, Hg) threatening both the environment and human health (Wang,  
2023; Zerizghi et al., 2022). For example, the activity of thermal power plants located to the east of  
65 South Africa, showed a four to five folds rise over the last decade owing to the increased demand of  
power generation (Morosele and Langerman, 2020; Zerizghi et al., 2022). (Morosele and Langerman,  
2020; Zerizghi et al., 2022) Similarly, both southern African countries and Madagascar have also  
recently experienced a steep increase in vehicle numbers, enhancing the vehicular and road emissions  
(Department of Transport, 2017; Iimi, 2023).

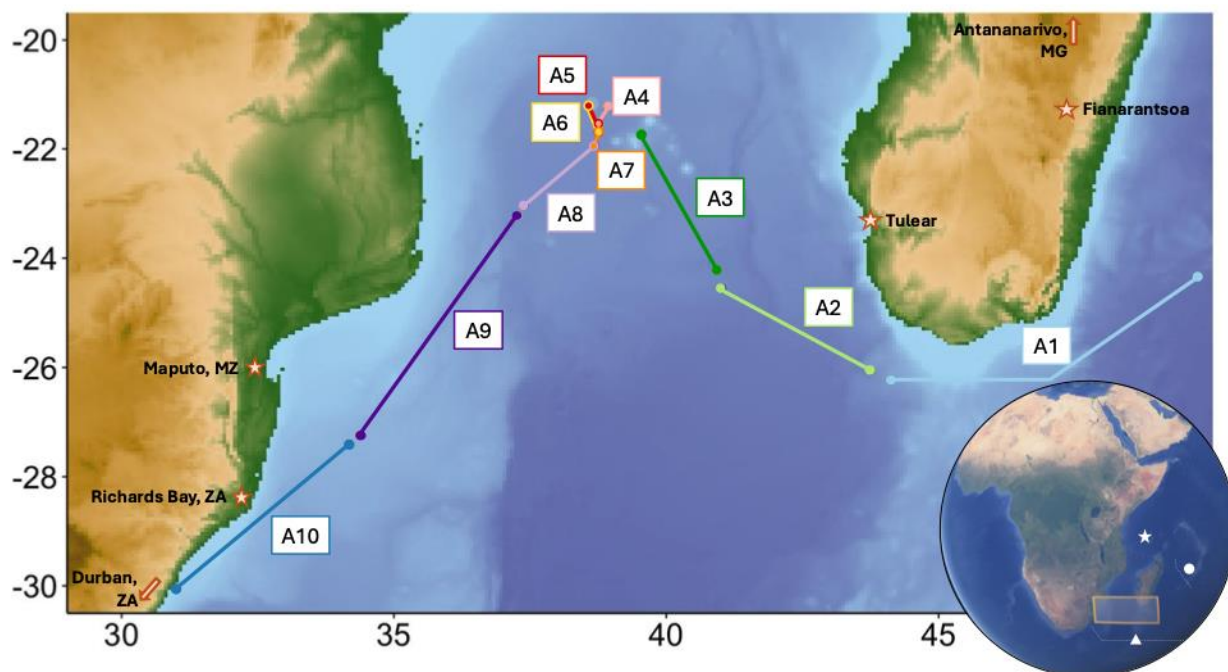
70 These anthropogenic activities emit not only nutrients but also toxic trace metals. Their finer particle  
size and emission processes can result in greater solubility upon deposition, making them potentially  
more bio-accessible (or more toxic) to micro-organisms than mineral dust (Sholkovitz et al., 2009).  
Mining and industrial hotspots, in the Highveld region of South Africa and near the cities of Richards  
Bay and Durban (South Africa) and Maputo (Mozambique) further contribute to the atmospheric burden  
75 of trace metals in the region.

Despite the diversity and intensity of surrounding natural and anthropogenic aeolian sources, no study to date has characterized the chemical composition of aerosols over the southern Mozambique Channel. Here, we present the first analysis of the atmospheric composition of trace elements, including aluminium (Al), Cd, chromium (Cr), copper (Cu), iron (Fe), nickel (Ni), Pb, titanium (Ti), vanadium (V), and zinc (Zn), based on aerosol samples collected during the late austral autumn (April-May) 2022 over the southern Mozambique Channel. Our objective is to provide an initial assessment of the chemical variability and source signatures of atmospheric inputs to this understudied marine system.

## 2 Materials and Methods

### 2.1 Aerosol collection during the RESILIENCE campaign

The RESILIENCE (fRonts, EddieS and marIne Life in the wEstern iNdian oCEan) campaign took place aboard the R/V Marion Dufresne II in the austral autumn 2022 with the aim to better understand small scale oceanic interactions between physics and biology within Mozambique Channel eddies and rings (Penven et al., 2025; Ternon et al., 2022). The cruise departed Reunion Island on the 19<sup>th</sup> of April 2022 to explore the central Mozambique Channel and sail along the southeast coast of South Africa to arrive in Durban on the 3<sup>rd</sup> of May 2022.



95 Figure 1. Location of the 10 aerosol samples, numbered A1 to A10, collected during the RESILIENCE cruise in the Southern Mozambique Channel. The inset world map indicates the location of this study (yellow rectangle) together with the location of previous field studies (symbols) reporting atmospheric trace element concentrations in the direct vicinity of our study region (triangle: Witt et al. (2006), circle: Witt et al. (2010), star: Chester et al. (1991).

Collection of atmospheric total suspended particles was undertaken using acid-cleaned Whatman 41 filters (Cutter et al., 2017; Morton et al., 2013) and a high-volume air sampler (TE-5170, Tisch Environmental, flow rate: 1.08m<sup>3</sup>/min). The aerosol sampler, installed on the upper viewing deck of the ship, roughly 18 m above the sea level, enabled the collection of ten 47 mm filters simultaneously. Sampling was only undertaken when the ship was underway and under front winds (290° - 70° relative to the ship's position) to prevent contamination from the ship's smokestack. Filter holder preparation and retrieval were undertaken under a laminar flow hood placed inside a "clean bubble" laboratory in the ship. Filters were collected every 24 hours, placed in clean petri dishes using plastic tweezers and stored frozen in double sealed bags until further analysis in the land-based laboratory. Two filter blank samples, consisting of acid washed Whatman 41 which were not brought to the field, were used for blank correction as described in section 2.2. The indicative location of aerosol sampling transects is displayed in Figure 1 and the supplementary material Table S1 provides a log-sheet of all 10 aerosol samples collected, including collection dates and associated ship's coordinates.

## 2.2 Aerosol trace element analysis

Laboratory work was carried out in a positive pressured class 6 clean room, in an HEPA-filtered class 5 laminar flow hood wearing clean garments and nitrile gloves and following GEOTRACES 'Cookbook' procedures (Cutter et al., 2017). All chemicals used were ultra-high purity grade solutions. To assess the soluble (S<sub>X</sub>) and total (T<sub>X</sub>) concentrations of each target metal ("X") in aerosols, sampled filters were processed through a sequential leaching protocol modified from Perron et al. (2020). Measurements of Al, Cd, Cr, Cu, Fe, Ni, Pb, Ti, V and Zn are discussed in this study. Briefly, aerosol samples were thawed at room temperature. Each filter was placed in a centrifuge tube, soaked for 2h in 10 mL of ammonium acetate (1.4 M, pH 4.7) then centrifuged at 4200 rpm for 3 minutes. The operationally defined soluble fraction of metal in aerosols, S<sub>X</sub>, was quantified in a 5 mL aliquot of the leachate solution following evaporation of the acetate buffer and redissolution of the residue into 0.15M nitric acid (HNO<sub>3</sub>). The residual 5mL of leachate together with the filter were evaporated to dryness and digested using a mixture of concentrated hydrofluoric acid (14M, HF, 0.25 mL) and HNO<sub>3</sub> (15M, 1mL) for 12 h at 120 °C. Following another round of HNO<sub>3</sub> (5mL, 7M) digestion and evaporation, the refractory fraction of metal in aerosols was quantified from a 5mL HNO<sub>3</sub> (0.3M) aliquot. Metal concentrations in aerosol leachates were determined by Sector Field Inductively Coupled Plasma Mass Spectrometer (SF-ICP-MS, Element XR) at the Pôle Spectrométrie Ocean (Brest, France). Indium (In, 10 ng g<sup>-1</sup>) was added as an internal standard in the analysed leachates to correct for potential instrumental drift during analysis. The average procedural blank was subtracted from the trace element mass measured in each leachate. The sum of measurements obtained in the two steps of the protocol defines the total fraction of trace metals in aerosols, T<sub>X</sub> (Perron et al., 2020). The digestion and analysis of two reference materials, namely the Arizona Test Dust (<3 µm, Powder Technologies Inc®) and the Bureau of Reference plankton certified reference material (BCR-414) alongside the samples provided satisfactory recovery for all trace metals presented in this study (see supplementary Table S2). Blank contributions to the sample measured concentrations were calculated for each leaching step and are displayed in the supplementary Table S3. The refractory fraction of metal in aerosol was, for some samples, below blank levels. These measurements, for which T<sub>X</sub> only

corresponds to  $S_X$  concentration in aerosols (see Table S4), are flagged in red in Tables and are excluded from subsequent calculations.

140 Concentrations of metals in aerosols are expressed in nanogram of metal “X” per cubic meter of air filtered ( $\text{ng m}^{-3}$ ). Aerosol fractional solubility is calculated as the ratio of soluble-to-total metal concentration ( $S_X/T_X$ ) in a sample expressed as a percentage.

### 2.3 Dust deposition flux estimate

145 Aluminium content measured in the collected aerosols was used to estimate lithogenic (dust) deposition flux ( $F_{\text{Dust}}$ ) in our study region.

Dust deposition was estimated assuming a prevailing crustal origin of Al and using the relative abundance of the metal,  $[\text{Al}]_{\text{UCC}}$ , in the upper continental crust (UCC) according to McLennan (2001). Based on assumptions made in previous studies (Baker et al., 2016; Marsay et al., 2022), a constant deposition velocity ( $V_d$ ) of  $1.2 \text{ cm s}^{-1}$  (or  $V_d = 1036.8 \text{ m d}^{-1}$ ) was used to calculate  $F_{\text{Dust}}$  following Eq. (1):

$$FDust = \frac{T_{\text{Al}} \times V_d}{[\text{Al}]_{\text{UCC}}} \times 365 \quad (1)$$

where  $T_{\text{Al}}$  is the total Al concentration measured in aerosols, and  $[\text{Al}]_{\text{UCC}} = 8.04\%_{\text{w/w}}$  (McLennan, 2001). The resulting  $FDust$  flux was expressed in  $\text{mg m}^{-2} \text{ yr}^{-1}$  by multiplying the daily flux by 365 days. As particle dry deposition velocity is sensitive to the particle size, the relative humidity, and wind speed, this parameter cannot be accurately calculated for each sampling period investigated. Hence, we acknowledge that uncertainty is associated with the use of a constant deposition velocity which was previously estimated to range by a factor of 2-3 (Duce et al., 1991; Marsay et al., 2022). Due to Al showing 100% solubility in the two lowest trace element mass loading samples A2 and A7 (suggesting significant influence from anthropogenic emissions), these two samples were excluded from the determination of  $F_{\text{Dust}}$  in our study.

## 2.4 Tracking the source of metal in aerosols

### 2.4.1 Air-mass back-trajectories

165 Air-mass back-trajectories (AMBT) were calculated for each aerosol sample mid-sampling location-to assess potential atmospheric source influence. The HYSPLIT model (Air Resources Laboratory, NOAA, Stein et al. (2015)) was run using R packages “Splitr” (Iannone, 2016) and “openair” (Carslaw and Ropkins, 2012) and Global Forecast System (GFS  $0.25^\circ \times 0.25^\circ$ ) meteorological data. AMBT were calculated 7 days back and at a height of 10m above the sea level. Cluster analysis was used to assess the proportion of major air-masses arriving at 3 key locations in our study region. Trajectories were run every 3 hours over the duration of the voyage at each of the 3 locations for cluster analysis. This analysis enabled to model the influence of less prevailing air-masses of terrestrial origin, which can have disproportionate influence on the particulate loading of marine aerosol samples and their elemental composition.

## 2.4.2 Enrichment factors

175 Enrichment factor (EF) is a common tool used to estimate the relative contribution of lithogenic versus anthropogenic source contained for each aerosol metal investigated. EFs were calculated as the ratio of total metal “X”-to-Al concentration measured in aerosols compared to the same ratio in the upper continental crust (UCC), following Eq. (2):

$$EF(X) = \frac{\frac{TX}{TAl} aerosol}{\frac{TX}{TAl} UCC} \quad (2)$$

180 Aluminium crustal content (Al, 8.04%<sub>ow/w</sub>, McLennan, 2001) was chosen as a reference in this study due to its reported prevailing lithogenic origin.

A threshold value of 10 was chosen, above which metal content in aerosols is deemed “enriched” by anthropogenic inputs (Shelley et al., 2015). Such threshold must be sufficiently high to account for natural variability across dust sources worldwide and natural fractionation processes occurring during the production, emission and transport of aerosols (Hird et al., 2024; Reimann and de Caritat, 2005). A  
185 the production, emission and transport of aerosols (Hird et al., 2024; Reimann and de Caritat, 2005). A minor and insignificant contribution of anthropogenic emissions can never be completely ruled out as it can be one of many factors resulting in the increase in one element’s EF over the expected crustal value of 1.

## 2.4.3 Statistical analysis

190 Pearson’s correlation test was performed to test for linear relationship between the total atmospheric concentration of paired trace elements. Supplementary Figure S3 summarizes the correlation factor calculated between each pair of elements as well as their degree of significance (p-value). In our study, Pearson’s r correlation factors were defined as very strong when ranging 0.8-1.0 (Strzelec et al., 2020), with a significant correlation set for p-value <0.01.

195

## 3. Results

### 3.1. Prevailing atmospheric transport during the RESILIENCE campaign

Typical single back-trajectory analysis of prevailing air-masses arriving at 10m altitude at the mid-sampling time and location of each sample collected during the RESILIENCE campaign are presented  
200 in the supplementary Figure S1. Such single trajectory analysis often highlighted a prevailing air-mass origin from long-range transport over the Southern Ocean, obscuring potential inputs from the two major landmasses present in our study region.

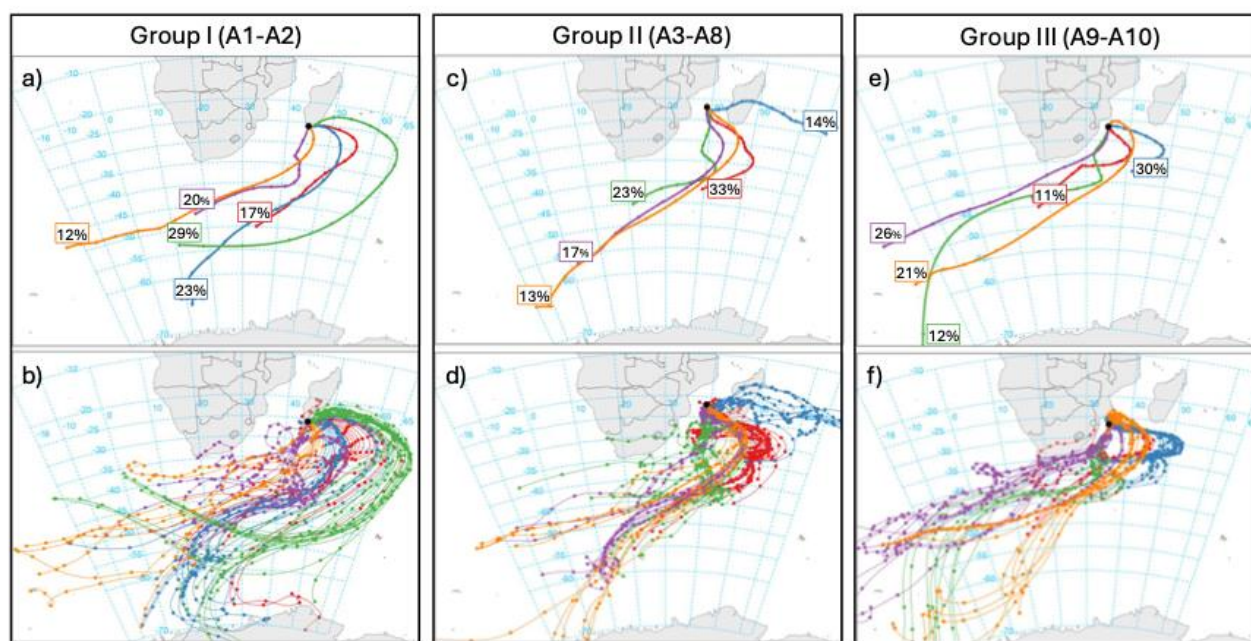
Since model observations suggest a decrease in atmospheric loading at lower latitude (<25° S) in our  
205 study region (Flamant et al., 2022; Gili et al., 2022; Jickells et al., 2005; Li et al., 2008a; Neff and Bertler, 2015), we divided our samples into three groups according to their locations (north vs south of 25° S and proximity to the two landmasses). Additional cluster analysis (Figure 2) was computed for the

2 groups of samples in order to account for the influence from less dominant yet higher loading terrestrial air-mass.

210 Group I and Group III consisted of aerosol samples collected south of 25° S, with the former sample group being collected at proximity to Madagascar (A1-A2, Figure 2a and 2b) and the latter, at proximity to southern Africa (A9-A10, Figure 2e and 2f). While Group I showed an influence from coastal air-masses originating from Madagascar (represented by the green, red and blue clusters in the Figure 2a and 2b), which accounted for up to 69% of the total incoming air-masses, Group III seemed to receive  
215 no influence from the island at all (Figure 2e and 2f).

Group II included samples A3-A8, collected at the centre of the Channel, north to 25° S, within a small sampling perimeter. Group II was characterised by a prevailing atmospheric influence from long-range transport of westerly winds across the Southern Ocean (accounting for up to 86% of the incoming air-masses as represented by the red, orange, purple and green clusters in Figure 2c and 2d). Sporadic  
220 terrestrial inputs from inland Madagascar Island were also observed in Group II aerosols, contributing 14% of the total incoming air-masses (blue cluster on the Figure 2c and 2d).

A more detailed characterisation of individual air-mass trajectories composing each cluster (Figure 2b, 2d, 2f) also emphasised additional influence of coastal Madagascar air-masses on Group I aerosols (represented by the red and orange clusters) which could be overlooked when solely accounting for the  
225 coarse cluster analysis outputs (Figure 2a, 2c, 2d). Similarly, in the detailed cluster analysis (Figure 2b, 2d, 2f), atmospheric inputs from southern Africa cannot be ruled out in any aerosol group.



230 **Figure 2. Seven day back-trajectory cluster analysis for the 5 prevailing air-masses arriving at 10m height at the middle location of each aerosol sample Group. Panels a), c) and e) represent the “coarse” cluster analysis including the contribution of each air-mass to the global atmospheric transport while panels b), d) and f) represent a “detailed” analysis including each air-mass trajectory and its associated cluster (colour code).**

### 3.2. Total aeolian trace element loading over the southern Mozambique Channel

Trace element concentrations measured in individual aerosols collected in our study and total trace  
 235 element mass loading data, defined as the sum of all 10 target element concentrations are reported in  
 Table 1. The trace element total mass loading in aerosols ranged from 5.0 to 87 ng m<sup>-3</sup>, with decreasing  
 metal contents in samples in the following order: A6>A8>A3>A9>A1>A4>A5>A10>A7>A2.  
 Interestingly, the trace element total mass loading measured in aerosols in our study showed a high  
 240 spatial variability with no hotspot for aeolian dust deposition identified and a seemingly random  
 distribution of high and low total mass loading across the sampling region, regardless of the sample  
 clusters defined above (aerosol sample Groups I, II and III).  
 Amongst the target metals, 99% of the trace element total mass loading in our samples was comprised  
 of Al, Cr, Cu, Fe, Ti, and Zn. These elements are subsequently referred to as “major” trace elements as  
 opposed to “minor” trace elements, which contributed less than remaining 1% of the total metal loading  
 245 in aerosols (i.e., Cd, Ni, Pb, and V).

**Table 1. Total concentration of “major” (Al, Cr, Cu, Fe, Zn, and Ti) and “minor” (Cd, Ni, Pb, and V) trace elements measured in aerosol samples (A1-A10) over the southern Mozambique Channel. Median and median absolute deviation (MAD) values are indicated in the last column. The sum of all 10 target element concentrations is displayed as the trace element total mass loading (TE loading).**

	A1	A2	A3	A4	A5	A6	A7	A8	A9	A10	Median± MAD
<i>Major trace elements, ng m<sup>-3</sup></i>											
Al	21.6	0.2*	35.8	11.5	8.5	55.9	3.0*	54.6	22.1	9.2	16±11
Cr	0.1	4.3	5.1	3.8	5.9	0.5	3.5	0.4	0.1	5.0	4±2
Cu	1.4	0.2	0.8	0.3	0.3	0.8	0.2	1.0	1.6	0.04	0.5±0.4
Fe	10.0	LQ	3.6	2.1	0.8	9.9	0.8	7.5	8.6	1.1	3±2
Ti	0.3	LQ	3.4	0.7	0.9	7.9	0.3	3.1	4.3	LQ	1±1
Zn	3.1*	0.2*	8.5*	6.4	0.5	11.8*	0.8*	15.4*	2.8*	0.2	3±3
<i>Minor trace elements, pg m<sup>-3</sup></i>											
Cd	21.3*	2.4*	141.8*	55.0*	13.4	172.3*	8.1*	233.7*	4.6	9.7	17±14
Ni	60.9	3.8	102.5	90.6	20.5	199.8	13.5*	210.2	58.3	14.8	60±44
Pb	34.2	3.0*	54.8	22.6	3.5	70.3	7.0	83.3	38.2	1.8	28±25
V	19.9	LQ	12.1	3.6	6.2	27.2	3.7*	21.9	20.2	3.4	9±7
<i>TE loading, ng m<sup>-3</sup></i>											
	36.7	5.0	57.5	25.0	17.0	87.3	8.7	82.5	39.6	15.6	

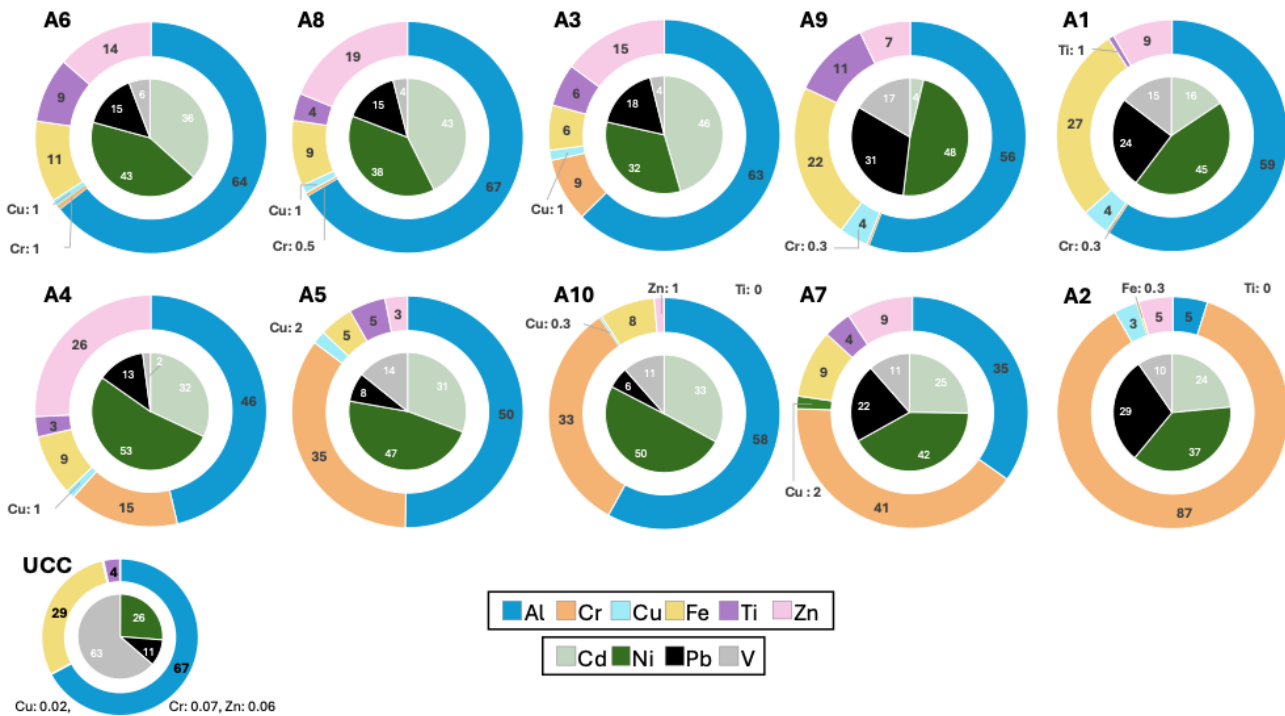
“\*” Soluble trace metal concentrations for which the refractory metal fraction was below procedural blank value.

“LQ” represents soluble trace metal concentrations which are below the analytical limit of quantification (defined as 10\*standard deviation of the analytical blank).

Trace element concentrations quantified in RESILIENCE aerosol samples ranged across four orders of  
 250 magnitude, from a few picograms to tens of nanograms per cubic meter of air. Amongst major trace  
 elements, the median concentration of Al (16±11 ng m<sup>-3</sup>) was at least 4 times greater than that of other

major elements. Median concentrations of Cr ( $4\pm 2 \text{ ng m}^{-3}$ ) were slightly higher than that of Fe ( $3\pm 2 \text{ ng m}^{-3}$ ) and Zn ( $3\pm 3 \text{ ng m}^{-3}$ ) while smaller concentrations were found for Ti ( $1\pm 1 \text{ ng m}^{-3}$ ) and Cu ( $0.5\pm 0.4 \text{ ng m}^{-3}$ ) across the range of samples collected over the southern Mozambique Channel. Amongst minor trace elements, Ni was the most abundant element (median:  $60\pm 44 \text{ pg m}^{-3}$ ), followed by Pb ( $28\pm 25 \text{ pg m}^{-3}$ ), Cd ( $17\pm 14 \text{ pg m}^{-3}$ ), V ( $9\pm 7 \text{ pg m}^{-3}$ ).

Samples A2 and A7 stood out due to their overall low trace element content. In these aerosols, a number of analysed trace elements were only found in a soluble form (except for Cr, Cu and Ni in A2 and for Cr, Cu, Fe, Ti and Pb in A7) and the total trace element mass loadings were lower than that of other aerosol samples. Soluble trace element contribution to individual aerosol samples is displayed in the supplementary Table S4.



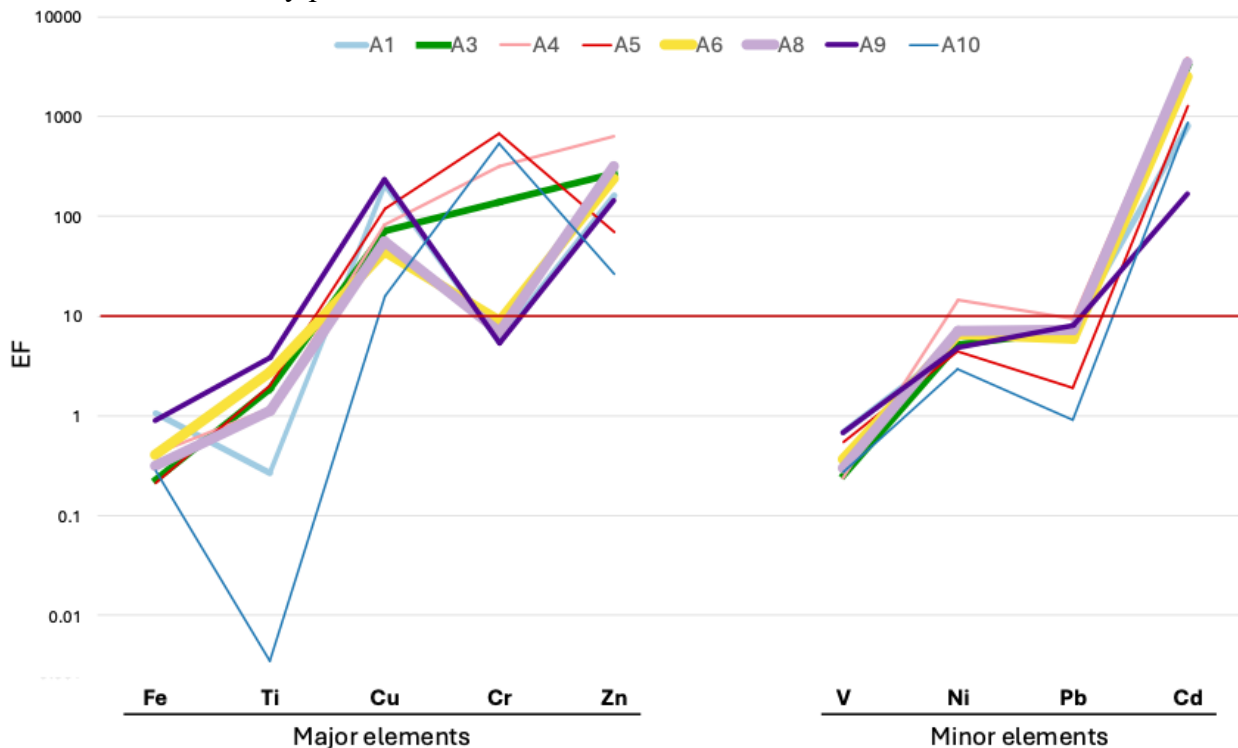
265 **Figure 3. Relative proportion (%) of total trace elements measured in aerosols (A1-A10) over the southern Mozambique Channel. The outer (inner) circle represents major (minor) trace elements composing over 99% (less than 1%) of the total trace element mass loading in individual samples. Samples are ordered according to decreasing total metal mass loading ( $A6 > A_x > A2$ ). The relative composition of the average UCC (McLennan, 2001) when accounting for the same metals is shown for comparison.**

270 Figure 3 offers a visual representation of the relative proportion of major and minor total trace elements measured in each aerosol sample collected over the Mozambique Channel. As a major trace element in this study, Al constituted over half of the total trace element loading (46 - 66%) in most aerosol samples collected except for A7 (35%) and A2 (5%). Higher Al abundance was found in samples with the highest total metal loading ( $A8 > A6 > A3$ ). Variable Fe and Ti content were found across aerosol samples with generally low relative Fe abundance compared to expected crustal average (UCC), except for A1

275 and A9. Contrastingly, high abundances were found for Cr, Cu and Zn, from 1 to 3 orders of magnitude higher than the average UCC. In particular, low total trace elements loading samples (A2, A7, A10 and A5) displayed extremely high Cr content, composing 33% up to 87% of the sample total trace element mass loading (Figure 3). Amongst the minor elements, high relative abundances in Cd and Ni were found, which contributed 0.01-0.3% and 0.08-0.4% of the total trace element mass loading, 280 respectively. Relative Pb content (0.01-0.1% of the total trace element mass loading) in RESILIENCE aerosols was higher than in the average UCC, especially in A1, A2, A7 and A9.

### 3.3 Tracking sources of trace metal in aerosols from the southern Mozambique Channel

285 Enrichment factors were calculated to assess the contribution from non-lithogenic sources to individual trace elements measured in aerosols collected over the southern Mozambique Channel (Figure 4 and supplementary Figure S2), except for samples A2 and A7 where they could not be determined as the Al content in the refractory phase was below the detection limit.



290 **Figure 4. Enrichment factors calculated for each trace element measured in individual aerosol samples collected over the southern Mozambique Channel. The thickness of the line is proportional to the total metal loading in aerosols. The horizontal red line indicates the significant enrichment threshold value of 10 used in this study.**

Amongst major elements, EFs close to 1 were found for Fe (median: 0.4) which indicated a prevailing lithogenic origin for Fe in all our aerosol samples (Figure 4). More variable EFs were calculated for Ti (median: 1.9); although values below the threshold of 10 also indicated a crustal origin for Ti in aerosols across the southern Mozambique Channel. Enrichment factors between 45 and 630 were found

295 for Cu (median: 72) and Zn (median: 239), suggesting a significant and likely prevailing anthropogenic  
origin of Cu and Zn in all aerosols collected in our study, except for A10. For these two elements,  
however, aerosol sample A10 was characterised by much lower EF values of 16 and 26, highlighting a  
different or less pronounced (yet prevailing) anthropogenic influence on this sample. Contrasting  
enrichment was obtained for Cr (median: 138), with EF values lower than 10 calculated for high total  
300 trace element mass loading samples (A1, A6, A8, and A9) and severe enrichment ranging 138 - 672  
found in low trace element total mass loading samples (A4, A5, and A10) as well as in A3 (Figure 4).  
This indicates that, while natural sources dominate the Cr content in high total trace element loading  
samples, with no or small (insignificant) anthropogenic inputs suggested, human-derived Cr emissions  
are likely to predominate the Cr content in low total trace element loading samples.

305 Amongst minor elements, V, Ni and Pb showed EFs lower than 10, with median values of 0.4, 5.2 and  
7.2, respectively (Figure 4). This indicated a prevailing crustal origin for the three metals in most  
aerosol samples (Reimann and de Caritat, 2005). While minor contribution from anthropogenic sources  
cannot be completely ruled out in the case of Ni and Pb, we consider this input insignificant with  
respect to the crustal contribution. Sample A4 represents one exception for which Ni enrichment exceed  
310 the threshold of 10 ( $EF_{Ni}=14$ ), highlighting non-negligible inputs from anthropogenic sources in this  
sample. Extremely high enrichments were found for Cd (median: 2529) in all samples, with a  
particularly high median  $EF_{Cd}$  value of 3248 calculated for samples of Group II (A3-A8), collected  
north of 25° S in the centre of the Channel when compared to Group I (A1) and Group III samples (A9  
and A10) which showed a median  $EF_{Cd}$  of 809.

315

## 4. Discussion

### 4.1 Dust deposition fluxes

The range of annual dust deposition flux calculated during the RESILIENCE cruise (40-263 mg m<sup>-2</sup> yr<sup>-1</sup>) falls within the low end of  $F_{Dust}$  reported by Earth System Models (ESM) (0 - 788 mg m<sup>-2</sup> yr<sup>-1</sup>) in the  
320 same 20° S-30° S area of the southern Mozambique Channel (Table 2). While ESM account for a yearly  
average  $F_{Dust}$ , our lower estimate is consistent with our study taking place at the beginning of the dry  
season (April-May), before the main dust and fire events which commonly occur from May to October  
on both Madagascar Island and the southern African continent (Archibald et al., 2010; Bhattachan et al.,  
2012; Ginoux et al., 2012). In addition, high precipitations associated with both the flood events in the  
325 Kwa-Zulu Natal region of South Africa in mid-April 2022 (Radio France, 2022) and the Jasmine  
tropical storm on the western coast of Madagascar in late April 2022 (Meteo France, 2022), could result  
in reduced dust entrainment in the atmosphere, in turn contributing to lower fluxes calculated during our  
study period. While we observe a large variability in our  $F_{Dust}$  estimates, the consistency between our  
values and the mean annual dust deposition fluxes reported by ESM in the 20° S-30° S region of the  
330 southern Mozambique Channel could imply either 1) a limited year-to-year variability in dust  
deposition over the southern Mozambique Channel or 2) a poor constraint on  $F_{Dust}$  estimates by ESM  
due to a paucity of data. These global models vary in spatial and temporal resolution and use different  
satellite and ground-based observations to validate their outputs which result in a large range of dust

deposition fluxes reported by different modelling studies (references in Table 2). For example, Wagener et al. (2008) used a global model output forced to fit the data obtained from two oceanographic campaigns, including around the Kerguelen Island plateau. A result from using limited observational data points to force the model seem to be an underestimate of atmospheric dust deposition at proximity from the emission sources on land. Additional field observations such those provided in our study and the use of new high-resolution satellite observation would help refining model outputs in this drastically under sampled study region where small-scale emission sources may prevail.

**Table 2. Median and median absolute deviation of the dust deposition fluxes ( $F_{Dust(AI)}$ ,  $mg\ m^{-2}\ yr^{-1}$ ) calculated based on Al concentrations measured in RESILIENCE aerosols (southern Mozambique Channel), compared to fluxes reported by models in the southern Mozambique Channel region. Sample A2 and A7 were excluded from  $F_{Dust}$  calculation due to negligible lithogenic inputs in these samples.**

	<b>This study</b> $F_{Dust(AI)}$	<sup>a</sup> Jickells et al. (2005)	<sup>b</sup> Li et al. (2008)	<sup>c</sup> Wagener et al. (2008)	<sup>d</sup> Xu and Weber (2021)	<sup>e</sup> Westberry et al. (2023)
Simulation year	2022	present day	1979-1998	2004-2005	unknown	2003-2016
Latitude						
20°-25°S	<b>169±95</b>	0-200	158-236	2-18	30-100	~183
>25°S	<b>101±2</b>	0-500	158-788	4-(36*)	100-316	91-(273*)

<sup>a</sup>(Jickells et al., 2005), <sup>b</sup>(Li et al., 2008b), <sup>c</sup>(Wagener et al., 2008), <sup>d</sup>(Xu and Weber, 2021) <sup>e</sup>(Westberry et al., 2023)

\*Values reported south of 30°S.

Our field-based mean  $F_{Dust}$  estimates are consistent with southern Africa being a smaller dust source to the ocean south of 20° S (Kok et al., 2021; Li et al., 2008a) compared to other provinces downwind of Australian dust sources (328  $mg\ m^{-2}\ yr^{-1}$ ; Hird et al., 2024) or that off the coast of South America (200 - 1200  $mg\ m^{-2}\ yr^{-1}$ ; Menzel Barraqueta et al., 2019). Model outputs displayed in Table 2 emphasise the south-eastwards transport of dust sources from the border junction of Namibia, Botswana and South Africa, across the African continent and into the southern Indian Ocean. Such atmospheric dust path is suggested to mostly reach latitudes south of 25° S or 30° S as depicted by high average  $F_{Dust}$  of 550  $mg\ m^{-2}\ yr^{-1}$  reported in March during a seagoing campaign along the 32° S parallel between 30 and 40° E (Grand et al., 2015). Studies also report a decreasing influence (of a factor 2-3) of southern African dust sources as we move north of 25°S into the southern Mozambique Channel (Flamant et al., 2022; Gili et al., 2022; Jickells et al., 2005; Li et al., 2008a; Neff and Bertler, 2015; Piketh et al., 2002). Higher  $F_{Dust}$  estimates south of 25° S were not observed in our study where, on the contrary, 1.7 times increase in the mean  $F_{Dust}$  in Group II aerosol samples (Table 2) further emphasises the absence of the southern Africa dust outflow signature at the time of our study. According to HYSPLIT AMBT analysis, the prevailing atmospheric transport influencing our samples originated from the transport of westerly air-masses over the Southern Ocean, with sporadic passage over Madagascar Island and/or southern Africa that would provide most of the particulate loading in our samples. It is possible that, outside the local dust season (May-October), the south-eastwards transport of dust from major southern African sources may be

absent or restricted to latitudes higher than 30° S and therefore cannot be considered as a source of dust to the Mozambique Channel. Our results corroborate findings by Freiman and Piketh (2002) that, despite 27% of the southern Africa atmospheric circulation reaches the Indian Ocean during the austral autumn, this air-mass is largely transported to the south of our study region (Freiman and Piketh, 2003). This conclusion highlights the important role of seasonality when comparing field-based measurements of dust fluxes to yearly average model estimates.

#### 4.2 Tracking potential sources of trace elements in aerosols

AMBT analysis suggested a few recent (<7 days) inputs of terrestrial air-masses (from South Africa and/or Madagascar Island) to the southern Mozambique Channel atmospheric loading. The trace element composition in our aerosols was tentatively used to identify specific local sources to the atmosphere coming from both neighbouring landmasses.

**Table 3. Comparison of the average total trace element concentration (pmol m<sup>-3</sup>) measured in all aerosols collected over the southern Mozambique Channel (this study) with existing ship-board aerosol trace element measurements in the surrounding region (locations shown in Figure 1).**

	southern Mozambique Channel, this study	<sup>a</sup> Southern Indian (open) Ocean	<sup>b</sup> Tropical (open) Indian Ocean	<sup>c</sup> North of Reunion Island	<sup>d</sup> offshore Durban (coast)
season	April (early dry)	November (wet)	May (dry)	November (wet)	March (wet)
site	-25° S, 38° E	-30° S, 65° E	-8° S, 45° E	-15° S, 60° E	-32° S, 32° E
Al	822±753	772	815	1200	300 - 3600
Cu	10±9	68	3	30	20 - 75
Cr	55±44	9	3	7	
Fe	80±73	484	286	200	1500
Ti	44±54	39			
Zn	76±82	29	6	100	200
Cd	0.6±0.8	0.1	0.05	0.09	0.2
Ni	1±1	9	2	10	18 - 53
Pb	0.2±0.1	0.9	1	3	1 - 6
V	0.2±0.2	1	1	0.8	

<sup>a</sup>(Ge et al., 2024), <sup>b</sup>(Chester et al., 1991), <sup>c</sup>(Witt et al., 2010), <sup>d</sup>(Witt et al., 2006).

Overall, average atmospheric trace element concentrations measured in this study were similar (Al, Cu, and Ti) or lower (Fe, Ni, Pb and V) than data reported for marine air-masses over the southern Indian Ocean (Table 3, Chester et al., 1991; Ge et al., 2024). This finding reinforced our AMBT analysis showing a predominant influence from long-range atmospheric transport of westerly winds from across the Southern Ocean (Figure 2). However, sporadic inputs of lithogenic Al, Fe, Ni, Pb, Ti and V (EF<10,

Figure 4) and anthropogenic Cu ( $EF_{Cu}=72$ , Figure 4) emissions from Madagascar and from southern Africa cannot be ruled out given the proximity of both landmasses and the extensive and increasing anthropogenic activity they hold (including copper mining and smelting activity in South Africa and Zambia, Makgetla et al., 2019; Nex and Kinnaird, 2019; Sikamo, 2016). Indeed, the more detailed  
385 analysis of air-mass back trajectory transport shows, for all 3 sample groups, instances (at least one air-mass) of air-mass crossing the southern African continent then travelling over the ocean before reaching our sampling position. Such a diluted atmospheric signal observed in our study is consistent with the southern Africa atmospheric recirculation pathway previously highlighted by Freiman and Piketh (2002). Higher concentrations of anthropogenic Zn ( $EF_{Zn}=239$ , Figure 4) in our samples resembled  
390 concentrations reported downwind of anthropogenic emission sources in the southwestern Indian Ocean (Witt et al., 2006, 2010). Major sources of anthropogenic Zn to the atmosphere include coal combustion, non-ferrous metal smelting and non-exhaust traffic emissions (Schleicher and Weiss, 2023; Wei et al., 2025). While no specific source could be pinpointed in our study using chemical fingerprinting or air-mass trajectory analysis, a large extent of coalfields in the eastern and northern  
395 regions of South Africa (Hancox and Götz, 2014; Nundze et al., 2024) could be a source of Zn to the southern Mozambique Channel north of  $25^{\circ}$  S (Group II aerosols), where Zn enrichment is overall 3 times higher than in Group I and Group III samples (except for sample A5). Indeed, air-mass trajectory analysis show existing trajectories (Figure 2 green line for group II and red line for group III samples), passing near the southernmost coalfield regions. While the coalfields located to the northeast of South  
400 Africa do not appear as clear sources in the air-mass trajectory analysis (Figure 2), these trajectories only represent clustered samples trajectories and do not represent the exact trajectories for air-masses included in each individual aerosol sample collected. Solid coal combustion is also widely used for cooking and heating, in a vast majority of Malagasy households (Dasgupta et al., 2013) as well as in South Africa townships (Balmer, 2007), although the magnitude of emissions linked to such practises remains uncertain (Keita et al., 2021; Marais and Wiedinmyer, 2016).  
405 Another source of Zn to the north of our study region could originate from metal smelting activities. Unlike Group I and III aerosol samples, a very strong and significant ( $p<0.01$ ) correlation between Zn, Cd and Cu was found in our Group II samples (Figure S3) similar to previously reported near smelter facilities (Kasongo et al., 2024; Taylor et al., 2010). In addition, industrial combustion of coal was  
410 previously associated with Pb-containing easily transported fine particles while smelters tend to release coarse particle-bound Pb which are easier to mitigate at the source and less likely to undergo long-range aeolian transport (Zhang et al., 2024). In our study, small concentrations and insignificant enrichments ( $EF<10$ ) of Pb in aerosols collected across the southern Mozambique Channel tend to support the role of smelter emissions as a source of atmospheric Zn, Cu and Cd rather than coal combustion emissions.  
415 Our results are in line with a modelling study by (Ito and Miyakawa, 2023) showing that emissions from metal production (smelting) is a major, and often overlooked, source of labile trace elements to the atmosphere over the Mozambique Channel, especially in fall when dust and pyrogenic sources are low. Most trace elements measured in Group II aerosols showed very strong and significant ( $p$ -value  $<0.01$ ) correlation to Al, except for Cr and Ti (supplementary Figure S3). Such a widespread correlation  
420 between lithogenic and anthropogenic elements highlights the complex atmospheric influence in our study region as depicted by our air-mass trajectory analysis (Figure 2). In aerosols collected south of  $25^{\circ}$  S (sample Groups I and III), less significant correlations were found between trace elements

investigated (Figure S3). This further highlight the difficulty of identifying a specific source of trace elements in aerosols collected in our study region in the absence of specific chemical tracers.

425

### 4.3 A remaining challenge: fingerprinting mining emissions in aerosols

Amongst all trace elements measured in this study, atmospheric Cr and Cd measurements in aerosols collected over the southern Mozambique Channel stood out, with concentrations 6-18 times and 3-12 times higher than that previously reported in the surrounding region (Table 3), respectively. Such

430

elevated metal loadings were likely associated with anthropogenic emissions as indicated by high median enrichment factors ( $EF_{Cr}=138$  and  $EF_{Cd}=3248$ , Figure 4) and suggested the prevalence of anthropogenic aeolian sources of Cr and Cd originating from the neighbouring land-masses to the southern Mozambique Channel rather than from long-range atmospheric transport. A negative correlation between Cr and Cd in our aerosol samples (Figure S3) suggests that two distinct

435

sources influence the atmospheric loading of these elements over the Mozambique Channel. High atmospheric loading in Cd and Cr in our samples may raise some concern as the two metals are known pollutants with acute toxicity to both humans (Csavina et al., 2012; Ericson et al., 2008) and ecosystems (Athar and Ahmad, 2002). More specifically, high soluble fractions of Cr measured in aerosol samples A7- A10 (supplementary Table S4) collected on the western part of the southern Mozambique Channel,

440

may indicate a predominance of Cr(VI) in the atmosphere which is carcinogenic (Świetlik et al., 2011). Widespread Cd enrichment was observed throughout our sampling region, with an average 4.6 times increase in  $EF_{Cd}$  values in Group II aerosols (A3-A8, Figure 4) compared to aerosols collected south of 25° S (sample Groups I and III). As suggested in section 4.2, Cd emissions from smelting activities have previously been linked to elevated aerosol enrichment ( $EF_{Cd/(Al)}>1000$ ) over the Atlantic Ocean (Shelley et al., 2015). In addition, extreme Cd enrichments relative to Fe ( $EF_{Cd/(Fe)}$ ) up to 18800 were also reported in dust samples collected around gold mine tailing storage facilities in the South African Witwatersrand Basin (Maseki et al., 2017). In our study, Cd enrichment factors relative to Fe exceeded 763 in nearly all our aerosol samples, except in A9. A further 10-fold increase in the median enrichment factor of Cd relative to Fe ( $EF_{Cd/Fe}=7766$ , Table 4) was found in aerosols from Group II compared to those of Group I and Group III ( $EF_{Cd/Fe}=763$ , Table 4), potentially suggesting a contribution from gold mining activities in South Africa or in Madagascar to the Cd atmospheric loading in the southern Mozambique Channel to the north of 25° S. Notably, elevated Cd concentrations have also previously been reported in squids, a known bioaccumulating species, in waters around Reunion Island (to the east of our study region), although the source of Cd in that study remained unidentified (Annasawmy et al., 2022).

445

450

455

Concerning Cr enrichments were observed in samples containing lower total metal mass loading (A4, A5, and A10) as well as in A3 (Figures 3 and 4). Elevated atmospheric Cr(VI) concentrations were previously associated with emissions from the ferrochrome industry in the Bushveld Igneous complex, South Africa (Venter et al., 2017). However, Venter and colleagues (2017) report a co-enrichment in Cr and Fe in aerosols which we do not observe in our samples. South Africa also holds 72–80% of the world's viable chromite ore reserves (Coetzee et al., 2020). Chromite rocks mined in Madagascar

460

(Grieco et al., 2014) and South Africa (Kleynhans et al., 2023) have typical Cr/Fe ratios of 1.5-2.9, which largely exceeds the Cr/Fe ratio of 0.0024 in the average UCC (McLennan, 2001). Similar or higher Cr/Fe ratios (>1.4) were found in our samples A3, A4, A5, A7 and A10), indicating that Cr mining emissions might be a major contributor to the aeolian Cr loading in the southern Mozambique Channel north of 25° S (A3-A8) and close to South African coastlines (A10). While chromite mines are mostly concentrated in the north of Madagascar and in the Bushveld Igneous complex in South Africa, HYSPLIT AMBT analyses associated with our samples only rarely (Madagascar) or never (Bushveld) crossed these sources (supplementary Figure 2 and Figure S1). It is possible that our ABMT analyses does not comprise all air-masses influencing our samples and that minor atmospheric inputs from high loading terrestrial air-masses remain overlooked. In addition, other unidentified source of Cr may be influencing the atmospheric loading in our study region. For example, in Richards Bay, South Africa, discharges from the industrial sector were linked to significant enrichment in Cr, and to a lesser extent in Cd and Cu in local sediment samples collected in the harbour (Izegaegbe et al., 2023). Chromium enrichment was also previously reported in airborne particulates associated with coal mines (Dubey et al., 2012), which could also be a source in our study region. On Madagascar Island, chromium contamination of soil and water streams were also reported as a result of tannery and textile wastewater (Rasoazanany et al., 2007). Overall, our results highlight the difficulty in tracking aerosol trace element source in aerosols in the absence of specific tracers.

**Table 4. Total atmospheric trace element concentration ratios (g/g) used in previous studies to trace specific anthropogenic sources in aerosols and their respective values in samples collected over the southern Mozambique Channel (this study). A2 was excluded due to extreme Fe and Cr solubility (100%) in this sample, which potentially bias the ratios displayed.**

Variable	Source	Reported values	A1	A3	A4	A5	A6	A7	A8	A9	A10
Cr/Fe	<sup>a,b</sup> Chromite mining	1.5-2.9	0.013	<b>1.4</b>	<b>1.8</b>	<b>7.4</b>	0.053	<b>4.3</b>	0.051	0.014	<b>4.5</b>
EF <sub>Cd(Fe)</sub>	<sup>c</sup> Gold mining	<18800	763	<b>14107</b>	<b>9291</b>	5990	6242	3538	<b>11117</b>	190	3084

<sup>a</sup>(Grieco et al., 2014), <sup>b</sup>(Kleynhans et al., 2023), <sup>c</sup>(Maseki et al., 2017)

## 480 Conclusion

The sub-equatorial region of southern Africa drastically suffers from climate change, with temperatures rising above the global average and increasing frequency of extreme weather events (e.g., droughts, floods, cyclones, fires). This region is also affected by rapid urbanization and industrialisation of lands (Scholes et al., 2015). Such a variety of natural and anthropogenic influences most likely contribute to the atmospheric composition of the region, introducing both (bio)essential and toxic elements into the atmosphere. This study provides chemical characterisation of the trace element composition in aerosols collected over the southern Mozambique Channel (20° S-30° S) during the austral autumn 2022, when dust deposition and fire occurrence are both low (Archibald et al., 2010; Bhattachan et al., 2012; Ginoux et al., 2012). We report a complex atmospheric circulation in the region. Indeed, while 7-day

490 single air-mass back-trajectory computed for each sample suggested a prevailing long-range transport of  
aerosols by westerly winds at latitudes  $>25^{\circ}$  S, a full understanding of the sources influencing the trace  
element loading over the southern Mozambique Channel could not be achieved without accounting for  
less prevailing and sporadic inputs from neighbouring sources in southern Africa and on Madagascar  
495 (through detailed cluster analysis). Our observation stresses the need to investigate the full complexity  
of atmospheric circulation (beyond single prevailing air-mass analysis) as less frequent, terrestrial air-  
masses can have disproportionate impact on the particulate loading (and trace element composition) of  
aerosols in low deposition marine region across the Southern Hemisphere. Atmospheric metal  
concentrations measured in our samples were similar (Al, Cu, and Ti) or smaller (Fe, Ni, Pb and V) than  
concentrations previously reported in marine air-masses downwind of Southern Hemisphere emission  
500 sources. This confirmed that our study occurred during the low deposition season and that  
concentrations presented for the above-mentioned trace elements can be considered as background (low  
end) aeolian concentrations. Trace elements commonly associated with crustal sources (Al, Fe, Ti)  
showed no significant enrichments relative to the averaged UCC ( $EF < 10$ ) neither did Ni, Pb, and V  
despite the three metals being sometimes related to human emissions in other studies. High  
505 concentrations of Zn (and elevated Cu enrichment factor) in aerosols were associated with  
anthropogenic emissions which could include coal combustion and smelting. Concentrations of Cd and  
Cr in our aerosol samples were 3 – 18 times higher than those reported in the literature near our study  
region and were associated with high Cr and extremely high Cd enrichments compared to the average  
UCC. Further analysis of atmospheric sources using elemental ratios in individual aerosol samples  
510 suggested inputs from mining activities (chromite: Cr, gold: Cd) to the atmosphere, especially in the  
central Channel between  $20^{\circ}$  S- $25^{\circ}$  S and close to the southern coastline of South Africa. While the  
atmospheric sources pointed out in our study are likely to run over the full year, time-series analysis of  
the identified chemical tracers' atmospheric loading is necessary to confirm such hypothesis. Our study  
emphasises the difficulty in tracking specific sources of atmospheric trace elements over marine regions  
515 due to the lack of defined atmospheric tracers for specific sources such as smelting and mining for  
example.

#### **Author contributions**

520 The study was conceptualised by EB, HP, AR. Funding was secured by EB and MMGP. Samples were  
collected by SS. Trace element analysis and data treatment were performed by MMGP, HP and YG and  
air-mass analysis and data interpretation were performed by TH. Data interpretation and early  
manuscript drafting were undertaken by MMGP, EB, HP and GS. All authors contributed to the final  
manuscript drafting.

### **Code and data availability**

525 All data produced for this study is available in the manuscript or as supplementary document. No  
dedicated code line was created for the purpose of this study although the following packages were used  
in RStudio : “openair”, “openairmaps”, and “splitr”.

### **Competing interests**

Authors declare that they have no conflict of interest.

530

### **Acknowledgements**

The RESILIENCE cruise was supported by the French National Oceanographic Fleet operated by  
Ifremer, by the Belmont Forum Ocean Front Change project, implemented through the French National  
Research Agency (ANR-20- BFOC-0006-04), by the ISblue project, Interdisciplinary graduate school  
535 for the blue planet (ANR-17-EURE-0015) and co-funded by a grant from the French government under  
the program “Investissements d’Avenir” embedded in France 2030, and by the French National  
program LEFE (Les Enveloppes Fluides et l’Environnement). Authors wish to thank S. Herbette, M.  
Noyon, P. Penven and J.-F. Ternon, P.I.s of the RESILIENCE MD#257 cruise (Ternon et al., 2022) and  
project and the crew of the R/V ‘Marion Dufresne’ (LDA, French Oceanographic Fleet) for their help  
540 and assistance. M.M.G.P was funded by a European Marie Skłodowska-Curie Actions fellowship  
number GA 101064063 and by an ISblue project, Interdisciplinary graduate school for the blue  
planet (ANR-17-EURE-0015) and co-funded by a grant from the French government under the program  
"Investissements d'Avenir" embedded in France 2030. Authors wish to thank insightful comments and  
545 literature suggestions from the two reviewers as well as from Dr Rebecca Garland which have  
significantly improved the discussion of this study.

## References

- Annasawmy, P., Bustamante, P., Point, D., Churlaud, C., Romanov, E. V., and Bodin, N.: Trace elements and  $\delta^{15}\text{N}$  values in micronekton of the south-western Indian Ocean, *Mar. Pollut. Bull.*, 184, 114053, <https://doi.org/10.1016/j.marpolbul.2022.114053>, 2022.
- 550 Archibald, S., Scholes, R. J., Roy, D. P., Roberts, G., and Boschetti, L.: Southern African fire regimes as revealed by remote sensing, *Int. J. Wildland Fire*, 19, 861–878, <https://doi.org/10.1071/WF10008>, 2010.
- Athar, R. and Ahmad, M.: Heavy Metal Toxicity: Effect on Plant Growth and Metal Uptake by Wheat, and on Free Living Azotobacter, *Water Air Soil Pollut.*, 138, 165–180, <https://doi.org/10.1023/A:1015594815016>, 2002.
- 555 Baker, A. R., Landing, W. M., Bucciarelli, E., Cheize, M., Fietz, S., Hayes, C. T., Kadko, D., Morton, P. L., Rogan, N., Sarthou, G., Shelley, R. U., Shi, Z., Shiller, A., and van Hulten, M. M. P.: Trace element and isotope deposition across the air–sea interface: progress and research needs, *Philosophical Transactions of the Royal Society A: Mathematical, Physical and Engineering Sciences*, 374, 20160190, <https://doi.org/10.1098/rsta.2016.0190>, 2016.
- 560 Balmer, M.: Household coal use in an urban township in South Africa, *Journal of Energy in Southern Africa*, 18, 27–32, <https://doi.org/10.17159/2413-3051/2007/v18i3a3382>, 2007.
- Barimalala, R., Wainwright, C., Kolstad, E. W., and Demissie, T. D.: The 2019–21 drought in southern Madagascar, *Weather Clim. Extrem.*, 46, 100723, <https://doi.org/10.1016/j.wace.2024.100723>, 2024.
- 565 Bhattachan, A., D’Odorico, P., Baddock, M. C., Zobeck, T. M., Okin, G. S., and Cassar, N.: The Southern Kalahari: a potential new dust source in the Southern Hemisphere?, *Environmental Research Letters*, 7, 024001, <https://doi.org/10.1088/1748-9326/7/2/024001>, 2012.
- Bhattachan, A., D’Odorico, P., and Okin, G. S.: Biogeochemistry of dust sources in Southern Africa, *J. Arid Environ.*, 117, 18–27, <https://doi.org/10.1016/j.jaridenv.2015.02.013>, 2015.
- 570 Carslaw, D. C. and Ropkins, K.: openair — An R package for air quality data analysis, *Environmental Modelling & Software*, 27–28, 52–61, <https://doi.org/10.1016/j.envsoft.2011.09.008>, 2012.
- Chester, R., Berry, A. S., and Murphy, K. J. T.: The distributions of particulate atmospheric trace metals and mineral aerosols over the Indian Ocean, *Mar. Chem.*, 34, 261–290, [https://doi.org/10.1016/0304-4203\(91\)90007-J](https://doi.org/10.1016/0304-4203(91)90007-J), 1991.
- 575 Coetsee, J. J., Bansal, N., and Chirwa, E. M. N.: Chromium in Environment, Its Toxic Effect from Chromite-Mining and Ferrochrome Industries, and Its Possible Bioremediation, *Expo. Health*, 12, 51–62, <https://doi.org/10.1007/s12403-018-0284-z>, 2020.
- Csavina, J., Field, J., Taylor, M. P., Gao, S., Landázuri, A., Betterton, E. A., and Sáez, A. E.: A review on the importance of metals and metalloids in atmospheric dust and aerosol from mining operations, *Science of The Total Environment*, 433, 58–73, <https://doi.org/10.1016/j.scitotenv.2012.06.013>, 2012.
- 580 Cutter, G. A., Casciotti, K., Croot, P., Geibert, W., Heimbürger, L.-E., Lohan, M. C., Planquette, H., and Flierdt, T. van de.: Sampling and Sample-Handling Protocols for GEOTRACES Cruises, Version 3.0, 2017.
- 585 Dasgupta, S., Martin, P., and Samad, H. A.: Addressing Household Air Pollution: A Case Study in Rural Madagascar., 2013.
- Department of Transport, S. A.: Annual Report for 2016/17 Financial Year Vote 35, 2017.

- Dubey, B., Pal, A. K., and Singh, G.: Trace metal composition of airborne particulate matter in the coal mining and non-mining areas of Dhanbad Region, Jharkhand, India, *Atmos. Pollut. Res.*, 3, 238–246, <https://doi.org/10.5094/APR.2012.026>, 2012.
- 590 Duce, R. A., Liss, P. S., Merrill, J. T., Atlas, E. L., Buat-Menard, P., Hicks, B. B., Miller, J. M., Prospero, J. M., Arimoto, R., Church, T. M., Ellis, W., Galloway, J. N., Hansen, L., Jickells, T. D., Knap, A. H., Reinhardt, K. H., Schneider, B., Soudine, A., Tokos, J. J., Tsunogai, S., Wollast, R., and Zhou, M.: The atmospheric input of trace species to the world ocean, *Global Biogeochem. Cycles*, 5, 595 193–259, <https://doi.org/10.1029/91GB01778>, 1991.
- Ericson, B., Hanrahan, D., and Kong, V.: *The World's Worst Pollution Problems: The Top Ten of the Toxic Twenty*, 2008.
- Flamant, C., Gaetani, M., Chaboureau, J.-P., Chazette, P., Cuesta, J., Piketh, S. J., and Formenti, P.: Smoke in the river: an Aerosols, Radiation and Clouds in southern Africa (AEROCLO-SA) case study, 600 *Atmos. Chem. Phys.*, 22, 5701–5724, <https://doi.org/10.5194/acp-22-5701-2022>, 2022.
- Frappier-Brinton, T. and Lehman, S. M.: The burning island: Spatiotemporal patterns of fire occurrence in Madagascar, *PLoS One*, 17, e0263313, <https://doi.org/10.1371/journal.pone.0263313>, 2022.
- Freiman, M. T. and Piketh, S. J.: Air Transport into and out of the Industrial Highveld Region of South Africa, *Journal of Applied Meteorology*, 42, 994–1002, [https://doi.org/10.1175/1520-0450\(2003\)042<0994:ATIAOO>2.0.CO;2](https://doi.org/10.1175/1520-0450(2003)042<0994:ATIAOO>2.0.CO;2), 2003.
- 605 Ge, Y., Guan, W., Wong, K. H., and Zhang, R.: Spatial Variability and Source Identification of Trace Elements in Aerosols From Northwest Pacific Marginal Sea, Indian Ocean and South Pacific to Antarctica, *Global Biogeochem. Cycles*, 38, <https://doi.org/10.1029/2024GB008235>, 2024.
- Gili, S., Vanderstraeten, A., Chaput, A., King, J., Gaiero, D. M., Delmonte, B., Vallelonga, P., 610 Formenti, P., Di Biagio, C., Cazanau, M., Panguì, E., Doussin, J.-F., and Mattielli, N.: South African dust contribution to the high southern latitudes and East Antarctica during interglacial stages, *Commun. Earth Environ.*, 3, 129, <https://doi.org/10.1038/s43247-022-00464-z>, 2022.
- Ginoux, P., Prospero, J. M., Gill, T. E., Hsu, N. C., and Zhao, M.: Global-scale attribution of anthropogenic and natural dust sources and their emission rates based on MODIS Deep Blue aerosol 615 products, *Reviews of Geophysics*, 50, <https://doi.org/10.1029/2012RG000388>, 2012.
- Grand, M. M., Measures, C. I., Hatta, M., Morton, P. L., Barrett, P., Milne, A., Resing, J. A., and Landing, W. M.: The impact of circulation and dust deposition in controlling the distributions of dissolved Fe and Al in the south Indian subtropical gyre, *Mar. Chem.*, 176, 110–125, <https://doi.org/10.1016/j.marchem.2015.08.002>, 2015.
- 620 Grieco, G., Merlini, A., Pedrotti, M., Moroni, M., and Randrianja, R.: The origin of Madagascar chromitites, *Ore Geol. Rev.*, 58, 55–67, <https://doi.org/10.1016/j.oregeorev.2013.11.002>, 2014.
- Hancox, P. J. and Götz, A. E.: South Africa's coalfields — A 2014 perspective, *Int. J. Coal Geol.*, 132, 170–254, <https://doi.org/10.1016/j.coal.2014.06.019>, 2014.
- Hird, C., Perron, M. M. G., Holmes, T. M., Meyerink, S., Nielsen, C., Townsend, A. T., de Caritat, P., 625 Strzelec, M., and Bowie, A. R.: On the use of lithogenic tracer measurements in aerosols to constrain dust deposition fluxes to the ocean southeast of Australia, *Aerosol Research*, 2, 315–327, <https://doi.org/10.5194/ar-2-315-2024>, 2024.
- Hooper, J. and Marx, S.: A global doubling of dust emissions during the Anthropocene?, *Glob. Planet. Change*, 169, 70–91, <https://doi.org/10.1016/j.gloplacha.2018.07.003>, 2018.

- 630 Iannone, R.: SplitR, <https://doi.org/doi.org/10.5281/zenodo.49106>, 2016.
- Iimi, A.: Estimating the demand for informal public transport: evidence from Antananarivo, Madagascar, *Public Transport*, 15, 129–168, <https://doi.org/10.1007/s12469-022-00300-9>, 2023.
- Ito, A. and Miyakawa, T.: Aerosol Iron from Metal Production as a Secondary Source of Bioaccessible Iron, *Environ. Sci. Technol.*, 57, 4091–4100, <https://doi.org/10.1021/acs.est.2c06472>, 2023.
- 635 Jickells, T. D., An, Z. S., Andersen, K. K., Baker, A. R., Bergametti, G., Brooks, N., Cao, J. J., Boyd, P. W., Duce, R. A., Hunter, K. A., Kawahata, H., Kubilay, N., laRoche, J., Liss, P. S., Mahowald, N., Prospero, J. M., Ridgwell, A. J., Tegen, I., and Torres, R.: Global Iron Connections Between Desert Dust, Ocean Biogeochemistry, and Climate, *Science (1979)*, 308, 67–71, <https://doi.org/10.1126/science.1105959>, 2005.
- 640 Kasongo, J., Alleman, L. Y., Kanda, J.-M., Kaniki, A., and Riffault, V.: Metal-bearing airborne particles from mining activities: A review on their characteristics, impacts and research perspectives, *Science of The Total Environment*, 951, 175426, <https://doi.org/10.1016/j.scitotenv.2024.175426>, 2024.
- Keita, S., Liousse, C., Assamoi, E.-M., Doumbia, T., N'Datchoh, E. T., Gnamien, S., Elguindi, N., Granier, C., and Yoboué, V.: African anthropogenic emissions inventory for gases and particles from 1990 to 2015, *Earth Syst. Sci. Data*, 13, 3691–3705, <https://doi.org/10.5194/essd-13-3691-2021>, 2021.
- 645 Kleynhans, E. L. J., Beukes, J. P., van Zyl, P. G., and du Preez, S. P.: Chemical beneficiation of chromite ore to improve the chromium-to-iron ratio for ferrochrome production, *Miner. Eng.*, 201, 108196, <https://doi.org/10.1016/j.mineng.2023.108196>, 2023.
- Kok, J. F., Adebisi, A. A., Albani, S., Balkanski, Y., Checa-Garcia, R., Chin, M., Colarco, P. R., 650 Hamilton, D. S., Huang, Y., Ito, A., Klose, M., Li, L., Mahowald, N. M., Miller, R. L., Obiso, V., Pérez García-Pando, C., Rocha-Lima, A., and Wan, J. S.: Contribution of the world's main dust source regions to the global cycle of desert dust, *Atmos. Chem. Phys.*, 21, 8169–8193, <https://doi.org/10.5194/acp-21-8169-2021>, 2021.
- Kumar, K. R., Sivakumar, V., Yin, Y., Reddy, R. R., Kang, N., Diao, Y., Adesina, A. J., and Yu, X.: 655 Long-term (2003–2013) climatological trends and variations in aerosol optical parameters retrieved from MODIS over three stations in South Africa, *Atmos. Environ.*, 95, 400–408, <https://doi.org/10.1016/j.atmosenv.2014.07.001>, 2014.
- Li, F., Ginoux, P., and Ramaswamy, V.: Distribution, transport, and deposition of mineral dust in the Southern Ocean and Antarctica: Contribution of major sources, *Journal of Geophysical Research: Atmospheres*, 113, <https://doi.org/10.1029/2007JD009190>, 2008a.
- 660 Li, F., Ginoux, P., and Ramaswamy, V.: Distribution, transport, and deposition of mineral dust in the Southern Ocean and Antarctica: Contribution of major sources, *Journal of Geophysical Research: Atmospheres*, 113, <https://doi.org/10.1029/2007JD009190>, 2008b.
- Mahlalela, P. T., Blamey, R. C., Hart, N. C. G., and Reason, C. J. C.: Drought in the Eastern Cape region of South Africa and trends in rainfall characteristics, *Clim. Dyn.*, 55, 2743–2759, <https://doi.org/10.1007/s00382-020-05413-0>, 2020.
- 665 Mahowald, N. M., Baker, A. R., Bergametti, G., Brooks, N., Duce, R. A., Jickells, T. D., Kubilay, N., Prospero, J. M., and Tegen, I.: Atmospheric global dust cycle and iron inputs to the ocean, *Global Biogeochem. Cycles*, 19, <https://doi.org/10.1029/2004GB002402>, 2005.
- 670 Makgetla, N., Levin, S., and Mtanga, S.: Moving up the copper value chain in Southern Africa, *UNU-WIDER*, <https://doi.org/10.35188/UNU-WIDER/2019/686-9>, 2019.

- Marais, E. A. and Wiedinmyer, C.: Air Quality Impact of Diffuse and Inefficient Combustion Emissions in Africa (DICE-Africa), *Environ. Sci. Technol.*, 50, 10739–10745, <https://doi.org/10.1021/acs.est.6b02602>, 2016.
- 675 Marsay, C. M., Kadko, D., Landing, W. M., and Buck, C. S.: Bulk Aerosol Trace Element Concentrations and Deposition Fluxes During the U.S. GEOTRACES GP15 Pacific Meridional Transect, *Global Biogeochem. Cycles*, 36, <https://doi.org/10.1029/2021GB007122>, 2022.
- Maseki, J., Annegarn, H. J., and Spiers, G.: Health risk posed by enriched heavy metals (As, Cd, and Cr) in airborne particles from Witwatersrand gold tailings, *J. South. Afr. Inst. Min. Metall.*, 117, 663–680 669, <https://doi.org/10.17159/2411-9717/2017/v117n7a8>, 2017.
- McLennan, S. M.: Relationships between the trace element composition of sedimentary rocks and upper continental crust, *Geochemistry, Geophysics, Geosystems*, 2, <https://doi.org/10.1029/2000GC000109>, 2001.
- Mendez, J., Guieu, C., and Adkins, J.: Atmospheric input of manganese and iron to the ocean: Seawater 685 dissolution experiments with Saharan and North American dusts, *Mar. Chem.*, 120, 34–43, <https://doi.org/10.1016/j.marchem.2008.08.006>, 2010.
- Menzel Barraqueta, J.-L., Klar, J. K., Gledhill, M., Schlosser, C., Shelley, R., Planquette, H. F., Wenzel, B., Sarthou, G., and Achterberg, E. P.: Atmospheric deposition fluxes over the Atlantic Ocean: a 690 GEOTRACES case study, *Biogeosciences*, 16, 1525–1542, <https://doi.org/10.5194/bg-16-1525-2019>, 2019.
- Meteo France: Madagascar : forte tempête tropicale Jasmine, 2022.
- Morosele, I. P. and Langerman, K. E.: The impacts of commissioning coal-fired power stations on air quality in South Africa: insights from ambient monitoring stations, *Clean Air Journal*, 30, <https://doi.org/10.17159/caj/2020/30/2.8833>, 2020.
- 695 Morton, P. L., Landing, W. M., Hsu, S., Milne, A., Aguilar-Islas, A. M., Baker, A. R., Bowie, A. R., Buck, C. S., Gao, Y., Gichuki, S., Hastings, M. G., Hatta, M., Johansen, A. M., Losno, R., Mead, C., Patey, M. D., Swarr, G., Vandermark, A., and Zamora, L. M.: Methods for the sampling and analysis of marine aerosols: results from the 2008 GEOTRACES aerosol intercalibration experiment, *Limnol. Oceanogr. Methods*, 11, 62–78, <https://doi.org/10.4319/lom.2013.11.62>, 2013.
- 700 Neff, P. D. and Bertler, N. A. N.: Trajectory modeling of modern dust transport to the Southern Ocean and Antarctica, *Journal of Geophysical Research: Atmospheres*, 120, 9303–9322, <https://doi.org/10.1002/2015JD023304>, 2015.
- Nex, P. A. M. and Kinnaird, J. A.: Minerals and Mining in South Africa, 27–35, [https://doi.org/10.1007/978-3-319-94974-1\\_4](https://doi.org/10.1007/978-3-319-94974-1_4), 2019.
- 705 Nundze, S., Ogunlaja, A., Eastwood, K., Thwala, M., and Melariri, P.: Investigation of nanomaterial and hazardous emissions at coal-fired power stations in Mpumalanga, South Africa, *S. Afr. J. Sci.*, 120, <https://doi.org/10.17159/sajs.2024/16062>, 2024.
- Paytan, A., Mackey, K. R. M., Chen, Y., Lima, I. D., Doney, S. C., Mahowald, N., Labiosa, R., and Post, A. F.: Toxicity of atmospheric aerosols on marine phytoplankton, *Proceedings of the National Academy of Sciences*, 106, 4601–4605, <https://doi.org/10.1073/pnas.0811486106>, 2009.
- 710 Penven, P., Ternon, J., Noyon, M., Herbette, S., Cambon, G., Comby, C., L'Hégaret, P., Malauene, B. S., Ménesguen, C., Nehama, F., Rauntenbach, G., Rufino, Y., and Sudre, F.: Characterizing the Central

- Structure of a Mesoscale Eddy-Ring Dipole in the Mozambique Channel From In Situ Observations, *J. Geophys. Res. Oceans*, 130, <https://doi.org/10.1029/2024JC021913>, 2025.
- 715 Perron, M. M. G., Strzelec, M., Gault-Ringold, M., Proemse, B. C., Boyd, P. W., and Bowie, A. R.: Assessment of leaching protocols to determine the solubility of trace metals in aerosols, *Talanta*, 208, <https://doi.org/10.1016/j.talanta.2019.120377>, 2020.
- Piketh, S. J., Swap, R. J., Maenhaut, W., Annegarn, H. J., and Formenti, P.: Chemical evidence of long-range atmospheric transport over southern Africa, *Journal of Geophysical Research: Atmospheres*, 107, <https://doi.org/10.1029/2002JD002056>, 2002.
- 720 Radio France: Debout la Terre: Inondations monstres en Afrique du Sud, 2022.
- Ranaivombola, M., Bègue, N., Vaz Peres, L., Fazel-Rastgar, F., Sivakumar, V., Krysztofiak, G., Berthet, G., Jegou, F., Piketh, S., and Bencherif, H.: Characterization of aerosol optical depth (AOD) anomalies in September and October 2022 over Skukuza in South Africa, *Atmos. Chem. Phys.*, 25, 3519–3540, <https://doi.org/10.5194/acp-25-3519-2025>, 2025.
- 725 Rasoazanany, E. O., Andriambololona, R., Andriannarivo, R. R., and Randriamanivo, L. V.: Pollution of the environment by tannery and textile waste waters in the areas of Antananarivo, Madagascar, 15 September 2007.
- Reimann, C. and de Caritat, P.: Distinguishing between natural and anthropogenic sources for elements in the environment: regional geochemical surveys versus enrichment factors, *Science of The Total Environment*, 337, 91–107, <https://doi.org/10.1016/j.scitotenv.2004.06.011>, 2005.
- 730 Richardson, D., Black, A. S., Irving, D., Matear, R. J., Monselesan, D. P., Risbey, J. S., Squire, D. T., and Tozer, C. R.: Global increase in wildfire potential from compound fire weather and drought, *NPJ Clim. Atmos. Sci.*, 5, 23, <https://doi.org/10.1038/s41612-022-00248-4>, 2022.
- 735 Rigden, A., Golden, C., Chan, D., and Huybers, P.: Climate change linked to drought in Southern Madagascar, *NPJ Clim. Atmos. Sci.*, 7, 41, <https://doi.org/10.1038/s41612-024-00583-8>, 2024.
- Schleicher, N. J. and Weiss, D. J.: Identification of atmospheric particulate matter derived from coal and biomass burning and from non-exhaust traffic emissions using zinc isotope signatures, *Environmental Pollution*, 329, 121664, <https://doi.org/10.1016/j.envpol.2023.121664>, 2023.
- 740 Scholes, B., Scholes, M., and Lucas, M.: *Climate Change: Briefings from Southern Africa*, Wits University Press, <https://doi.org/10.18772/22015119186>, 2015.
- Shelley, R. U., Morton, P. L., and Landing, W. M.: Elemental ratios and enrichment factors in aerosols from the US-GEOTRACES North Atlantic transects, *Deep Sea Research Part II: Topical Studies in Oceanography*, 116, 262–272, <https://doi.org/10.1016/j.dsr2.2014.12.005>, 2015.
- 745 Sholkovitz, E. R., Sedwick, P. N., and Church, T. M.: Influence of anthropogenic combustion emissions on the deposition of soluble aerosol iron to the ocean: Empirical estimates for island sites in the North Atlantic, *Geochim. Cosmochim. Acta*, 73, 3981–4003, <https://doi.org/10.1016/j.gca.2009.04.029>, 2009.
- Sikamo, J.: Copper mining in Zambia - history and future, *J. South. Afr. Inst. Min. Metall.*, 116, 491–496, <https://doi.org/10.17159/2411-9717/2016/v116n6a1>, 2016.
- 750 Stein, A. F., Draxler, R. R., Rolph, G. D., Stunder, B. J. B., Cohen, M. D., and Ngan, F.: NOAA’s HYSPLIT Atmospheric Transport and Dispersion Modeling System, *Bull. Am. Meteorol. Soc.*, 96, 2059–2077, <https://doi.org/10.1175/BAMS-D-14-00110.1>, 2015.
- Strzelec, M., Proemse, B. C., Barmuta, L. A., Gault-Ringold, M., Desservettaz, M., Boyd, P. W., Perron, M. M. G., Schofield, R., and Bowie, A. R.: Atmospheric Trace Metal Deposition from Natural

- 755 and Anthropogenic Sources in Western Australia, *Atmosphere (Basel)*, 11, 474,  
<https://doi.org/10.3390/atmos11050474>, 2020.
- Swap, R. J., Annegarn, H. J., and Otter, L.: Southern African Regional Science Initiative (SAFARI 2000): summary of science plan, *S. Afr. J. Sci.*, 98, 119–124, 2002.
- Swap, R. J., Annegarn, H. J., Suttles, J. T., King, M. D., Platnick, S., Privette, J. L., and Scholes, R. J.:  
760 Africa burning: A thematic analysis of the Southern African Regional Science Initiative (SAFARI 2000), *Journal of Geophysical Research: Atmospheres*, 108, <https://doi.org/10.1029/2003JD003747>, 2003.
- Świetlik, R., Molik, A., Molenda, M., Trojanowska, M., and Siwec, J.: Chromium(III/VI) speciation in urban aerosol, *Atmos. Environ.*, 45, 1364–1368, <https://doi.org/10.1016/j.atmosenv.2010.12.001>, 2011.
- 765 Taylor, M. P., Mackay, A. K., Hudson-Edwards, K. A., and Holz, E.: Soil Cd, Cu, Pb and Zn contaminants around Mount Isa city, Queensland, Australia: Potential sources and risks to human health, *Applied Geochemistry*, 25, 841–855, <https://doi.org/10.1016/j.apgeochem.2010.03.003>, 2010.
- Ternon, J.-F., Herbette, S., Penven, P., and Noyon, M.: RESILIENCE cruise, RV Marion Dufresne, <https://doi.org/10.17600/18001917>, 2022.
- 770 Thiagarajan, V., Nah, T., and Xin, X.: Impacts of atmospheric particulate matter deposition on phytoplankton: A review, *Science of The Total Environment*, 950, 175280, <https://doi.org/10.1016/j.scitotenv.2024.175280>, 2024.
- Wagener, T., Guieu, C., Losno, R., Bonnet, S., and Mahowald, N.: Revisiting atmospheric dust export to the Southern Hemisphere ocean: Biogeochemical implications, *Global Biogeochem. Cycles*, 22,  
775 <https://doi.org/10.1029/2007GB002984>, 2008.
- Wang, J.: The Economic and Environmental Effects of Coal Mining: South Africa, *Highlights in Business, Economics and Management*, 5, 86–95, <https://doi.org/10.54097/hbem.v5i.5025>, 2023.
- Wei, T., Dong, Z., Li, F., Kang, S., and Qin, X.: Quantifying the distribution and origins of aerosol zinc across the Northern Hemisphere using stable zinc isotopes: A review, *J. Hazard. Mater.*, 491, 137828,  
780 <https://doi.org/10.1016/j.jhazmat.2025.137828>, 2025.
- Westberry, T. K., Behrenfeld, M. J., Shi, Y. R., Yu, H., Remer, L. A., and Bian, H.: Atmospheric nourishment of global ocean ecosystems, *Science (1979)*, 380, 515–519, <https://doi.org/10.1126/science.abq5252>, 2023.
- Witt, M., Baker, A., and Jickells, T.: Atmospheric trace metals over the Atlantic and South Indian  
785 Oceans: Investigation of metal concentrations and lead isotope ratios in coastal and remote marine aerosols, *Atmos. Environ.*, 40, 5435–5451, <https://doi.org/10.1016/j.atmosenv.2006.04.041>, 2006.
- Witt, M. L. I., Mather, T. A., Baker, A. R., De Hoog, J. C. M., and Pyle, D. M.: Atmospheric trace metals over the south-west Indian Ocean: Total gaseous mercury, aerosol trace metal concentrations and lead isotope ratios, *Mar. Chem.*, 121, 2–16, <https://doi.org/10.1016/j.marchem.2010.02.005>, 2010.
- 790 Xu, H. and Weber, T.: Ocean Dust Deposition Rates Constrained in a Data-Assimilation Model of the Marine Aluminum Cycle, *Global Biogeochem. Cycles*, 35, <https://doi.org/10.1029/2021GB007049>, 2021.
- Zerizghi, T., Guo, Q., Zhao, C., and Okoli, C. P.: Sulfur, lead, and mercury characteristics in South Africa coals and emissions from the coal-fired power plants, *Environ. Earth Sci.*, 81, 116,  
795 <https://doi.org/10.1007/s12665-021-10046-5>, 2022.

Zhang, J., Sun, X., Wu, Q., Deng, J., Li, Z., Wen, M., Xu, L., Gu, Y., Han, T., Feng, L., and Duan, L.: Emission characteristics of lead and particulate matter from lead and zinc smelters in China, *J. Hazard. Mater.*, 476, 135224, <https://doi.org/10.1016/j.jhazmat.2024.135224>, 2024.

800 Zhou, W., Li, Q. P., and Wu, Z.: Coastal phytoplankton responses to atmospheric deposition during summer, *Limnol. Oceanogr.*, 66, 1298–1315, <https://doi.org/10.1002/lno.11683>, 2021.